Microelectronic Engineering 121 (2014) 122–126

Contents lists available at ScienceDirect

Microelectronic Engineering

journal homepage: www.elsevier.com/locate/mee

Electron Beam Induced Deposition on graphene on silicon oxide and hexagonal boron nitride: A comparison of substrates

S. Hari [a,*], A.M. Goossens [b], L.M.K. Vandersypen [b], C.W. Hagen [a]

[a] Delft University of Technology, Fac. Appl. Sciences, Charged Particle Optics Group, Lorentzweg 1, 2628 CJ Delft, The Netherlands
[b] Delft University of Technology, Kavli Institute of Nanoscience, Lorentzweg 1, 2628 CJ Delft, The Netherlands

ARTICLE INFO

Article history:
Received 28 October 2013
Received in revised form 16 April 2014
Accepted 24 April 2014
Available online 5 May 2014

Keywords:
Graphene
Substrate
Silicon oxide
Hexagonal boron nitride
Electron Beam Induced Deposition
Raman spectroscopy

ABSTRACT

Graphene, a monolayer of carbon atoms arranged in a hexagonal lattice, is an interesting material because of its unique electronic properties. Electron Beam Induced Deposition (EBID) is an attractive direct-write technique to fabricate graphene devices for electronic applications, due to the combination of the high resolution and the versatility of the technique. We study electron induced damage to graphene at the typical EBID energy and dose range. In particular, we investigate the role of the substrate by carrying out electron exposure studies of graphene on two different substrates – silicon oxide and hexagonal boron nitride. Raman measurements reveal the emergence of a disorder D peak upon irradiation of graphene on silicon oxide, whereas graphene on boron nitride does not show this damage. Further, we pattern structures on graphene using EBID from the platinum precursor $MeCpPtMe_3$ and analyze the changes in the Raman spectrum of graphene coming about due to electron stimulated effects in the presence of the precursor.

1. Introduction

Graphene is a material with several interesting electronic properties such as tuneable conductivity, room temperature quantum Hall effect [1] and high thermal conductivity [2,3], as well as several applications in industry. However, samples with high electronic quality are needed to realize this potential and they are not trivial to fabricate. Devices are typically made using lithography which enables the patterning of high resolution contacts but may leave behind contamination due to the use of resist, decreasing the electronic quality. Other techniques such as shadow mask evaporation avoid the use of resist but are limited in the resolution that can be achieved. Direct-write deposition of contacts by Electron Beam Induced Deposition (EBID) [4,5] holds the promise of combining the best of both methods when fabricating graphene devices for electronic measurements. Two and three dimensional nanostructures can be deposited by focusing an electron beam on a substrate onto which precursor molecules have been adsorbed. The process is carried out in a Scanning Electron Microscope. Decomposition of the molecules by the electron beam results in the non-volatile fragments forming a deposit on the substrate, while the volatile fragments are pumped out of the system. Various materials can be deposited by using appropriate precursor gases [5].

The electron energy used in EBID is typically 5 keV, much lower than the 100 keV used in resist based electron beam lithography (EBL), so no knock-on damage due to the beam is expected in EBID. However, the electron doses required for a typical EBID process are 20 $nC/\mu m^2$, as compared to 10 $pC/\mu m^2$ for EBL. Recently, several groups have reported possible damage to graphene samples due to electron exposure [6–13]. To characterize the effect of electron irradiation on graphene Raman spectroscopy is frequently used. A typical Raman spectrum of single layer graphene shows only a few prominent features, the G peak at ~1580 cm^{-1} and the 2D peak at ~2685 cm^{-1}. Disorder, as could be introduced by electron exposure, gives rise to a D peak at 1345 cm^{-1}. Teweldebrhan and Balandin [6] have reported the appearance of the D peak in graphene on Si/SiO_x after an electron dose as low as 0.02 $nC/\mu m^2$, using beam energies ranging from 5 keV to 20 keV. They also observed a broadening of the characteristic G peak and the D peak under irradiation. Upon increasing the dose, up to a maximum of 1 $nC/\mu m^2$, they observed that the D peak increased in intensity, attained a maximum and then decreased and saturated. The various stages in this evolution have further been explained in analogy with graphite, in terms of the amorphization trajectory for carbon materials proposed in [14]. The first stage, corresponding to an increase in intensity of the D peak, is attributed to the transformation of the crystalline lattice of graphene into nanocrystalline (nc) carbon. The second stage is attributed to the conversion of nc carbon into amorphous sp2 carbon. This explanation was further

* Corresponding author. Tel.: +31 152788161.
E-mail address: s.hari-1@tudelft.nl (S. Hari).

http://dx.doi.org/10.1016/j.mee.2014.04.037
0167-9317/

verified by current–voltage measurements demonstrating an increase in the resistance of the flake during these two stages.

Childres et al. [7] have studied the effect of electron beam irradiation on the electronic transport properties of graphene devices on Si/SiO_x substrates, and performed Raman measurements of the samples after each exposure as well. They report a decrease in the Charge Neutrality Point (CNP, defined as where the conductivity is a minimum) and carrier mobility, as well as the appearance of the D peak in the Raman spectrum upon electron exposure. The experiments were performed with a beam energy of 30 keV and the maximum dose used was 0.6 nC/μm^2 i.e. in the same dose range as [6]. They propose that the cause of this damage is the trapping of holes generated by the interaction of the beam with the substrate, at the Si/SiO_x interface, leading to an electron doping in graphene. They also found that the decrease in the CNP was negligible when using suspended graphene samples, confirming that the Si/SiO_x substrate played a role.

The substrate playing a role has also been suggested by Xu et al. [8]. They studied the evolution of the Raman spectrum of graphene on Si/SiO_x upon irradiation with a 10 keV beam, but for much higher doses $\sim$ 56 $\mu C/\mu m^2$. In addition to the appearance of the D peak, they observed for the first time that the G peak became much larger in intensity than the 2D peak. Using temporal Auger electron spectroscopy they were able to conclude that electron beam irradiation could decompose the underlying SiO_x substrate, creating mobile oxygen atoms which attack the graphene. This suggests a different mechanism of damage at higher doses than the one proposed in [6].

Electron exposure of graphene at intermediate electron doses, typical for EBID, was reported by Michalik et al. [9]. They used EBID to pattern Cobalt contacts on graphene on a Si/SiO_x substrate, using an electron dose of approximately 20 nC/μm^2 and a beam energy of 10 keV. The post-deposition Raman spectrum of the graphene showed a disorder-induced D peak up to 2 mm away from the region of deposition, as well as a 2D/G ratio smaller than 1. The latter is remarkable because it is observed at much smaller dose than used in [8].They also observed that the largest D/G ratio was not at the point of electron exposure (or deposition), but at the point of maximum precursor flux. They report this damage to be almost completely reversible upon annealing, and argue that this removes attached precursor molecules from the surface. Interestingly no damage of the graphene was seen when exposing it to the precursor gas only, without electron exposure.

So far the literature does not provide a clear mechanism for electron induced damage to graphene. For free-standing graphene, it is well established by measurements in a transmission electron microscope that damage to the lattice occurs only for electron energies above 80 keV [15]. For graphene on a substrate, however, the situation is less clear. At low electron doses, typically 20 times smaller than required for EBID, it is proposed in [6] that the damage comes about due to amorphization and is irreversible for doses higher than 0.05 nC/μm^2, whereas in [10] it is attributed to hydrogenation of graphene which is found to be reversible upon annealing, and in [7] the Si/SiO_x substrate was proposed to play a role. At very high electron doses, three orders of magnitude larger than required for EBID, it is suggested in [8] that the decomposition of the underlying SiO_x has an important role to play in the damage observed. And for an electron dose typical for EBID it is suggested in [9] that the precursor gas in combination with electron exposure plays a role, but that the observed damage is largely reversible upon annealing.

The objective of this paper is to study the effect of electron irradiation, at a typical EBID dose, on single layer graphene on two different substrates, SiO_x and hexagonal Boron Nitride (hBN). Raman spectroscopy is used to characterize the graphene quality before and after electron exposure. And finally the effect of patterning structures on graphene on hBN using EBID is presented.

2. Experimental details

Three different graphene samples were used in this study.

Sample I: The graphene samples were prepared by mechanical exfoliation from a graphite crystal and deposited on a silicon chip with a standard 285 nm thick oxide layer.

Sample II: Graphene was prepared by mechanical exfoliation and transferred with a wet transfer method [16] to a hexagonal boron nitride substrate [17]. The graphene was shaped into a Hall bar by defining a PMMA mask with e-beam lithography and etching with an oxygen plasma process. This etching process was not intentionally performed for the experiments presented in this paper. Moreover it does not change the intrinsic properties of graphene. As a last step the sample was annealed at 400 °C in an Ar/H_2 environment.

Sample III: Graphene was grown on a copper substrate by chemical vapor deposition. Polymer was spincoated on top of the graphene and the copper was etched away. The polymer/graphene stack was dried and transferred on top of a SiO_x wafer covered with thin hexagonal boron nitride crystals. Subsequently the sample was annealed at 400 °C in Ar/H_2 environment.

The electron exposure was performed with the help of a Quanta 3D FEG Dual Beam system using a 5 keV beam and a current of 25 pA measured with a Faraday cup. The pressure in the chamber was maintained at $1{\cdot}10^{-6}$ mbar. Since our goal is to understand the effect of the electron beam during the EBID process, it was not the entire flake that was subjected to a uniform dose, but only the area to be patterned. The other areas of the flake are, however, subjected to the secondary and backscattered electrons that are generated as a result of the interaction of the 5 keV electron beam with the substrate. These electrons have a range of energies and the exact dose deposited as a function of position is not known, but is estimated to be at least 4 orders of magnitude lower than the primary electron dose. This is based on the estimated size of the substrate area from which the backscattered electrons are emitted (typically microns) compared to the primary electron beam size (1–10 nm typically). The parameters for electron beam exposure were similar to those used in a typical EBID experiment, i.e. a dose of 20 nC/μm^2. This dose applies to all experiments reported here.

The Raman spectra were recorded using a Renishaw spectrometer under 514 nm laser excitation. The laser power was kept below 2 mW to avoid local heating.

3. Results and discussion

A total area of 25 μm^2 was exposed to a dose of 20 nC/μm^2 which was provided by scanning the beam several times over this area. Fig. 1a shows an AFM image of the graphene flake on Si/SiO_x (sample I) after electron beam exposure. The black regions were irradiated by the electron beam. The blue spot shows the point where the Raman spectrum was acquired. Fig. 1b shows the Raman spectrum of sample I before and after electron irradiation. Both spectra are normalized to the silicon peak at 520 cm^{-1}. However, the noise level in the post irradiation spectrum is higher than that of the pristine sample as a result of the total counts being lower. In the spectrum of the pristine sample, the characteristic G and 2D peaks of graphene are clearly visible at 1589 cm^{-1} and 2685 cm^{-1} respectively. The peaks at approximately 520 cm^{-1} and 960 cm^{-1} are from the underlying silicon. The post-electron exposure Raman spectrum, on the other hand, shows the emergence of a D peak at 1345 cm^{-1}, which is known to arise due to structural disorder in

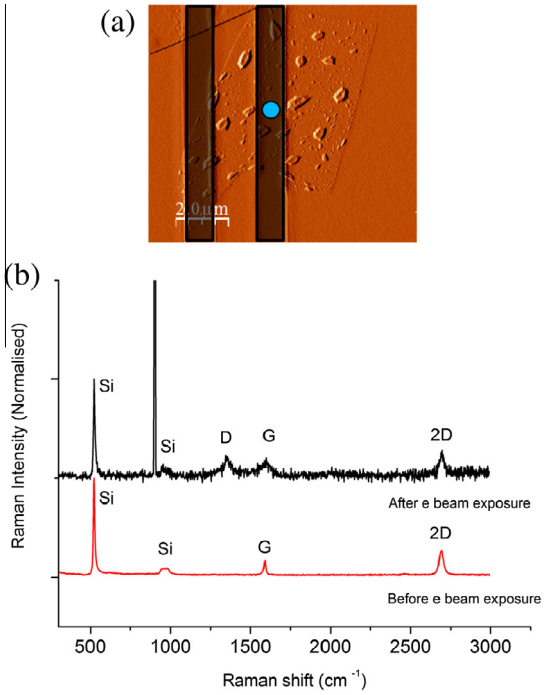

Fig. 1. (a) AFM image of the graphene flake (sample 1) after electron beam exposure. The black region was irradiated by the electron beam. The spot (shown in blue online) shows the point where the Raman spectrum was acquired. (b) Raman spectrum of the graphene flake (sample 1) before and after electron exposure. (For interpretation of the references to color in this figure legend, the reader is referred to the web version of this article.)

the graphene lattice [18,19]. This disorder is particularly significant since the D/G intensity ratio is approximately 1. (The peak at 902 cm^{-1} is the result of a spike in the detector readout and should be ignored). In addition, although the G and 2D peaks are still visible, the G peak is slightly shifted to 1597 cm^{-1} and is considerably broadened, with a FWHM approximately three times that of the pristine sample. This could be explained by a possible contribution from the D' peak at 1620 cm^{-1} which is also known to appear as a consequence of electron beam induced disorder [6]. This led us to believe that exposure to the electron beam with a typical EBID dose resulted in damaging the graphene on SiO_x.

It is evident from the literature that the possible mechanisms of damage include the influence of the Si/SiO_x substrate. Structural changes in the graphene brought about by its deformation on SiO_x could render it more susceptible to electron induced defects. Another possibility, mentioned before, is the reaction of graphene with mobile oxygen atoms created by decomposition of the SiO_x substrate under electron beam irradiation. In addition, studies on oxidative doping [20] suggest that the presence of charged impurities in the Si/SiO_x substrate leads to enhanced reactivity of graphene supported on SiO_x. This mechanism could also add to the damage in graphene under electron beam exposure. It is therefore interesting to investigate the results of a similar irradiation experiment on a different substrate. Hexagonal boron nitride (hBN) is of particular interest since it was shown to permit high carrier mobility graphene devices [17]. hBN is also known to have a number of more favorable properties than SiO_x for graphene based electronics, such as being isostructural with graphene with only a 1.7% lattice mismatch [21], containing no dangling bonds or surface charge traps. In addition, the absence of oxygen atoms eliminates at least a few of the damage mechanisms listed previously. We decided to use hBN as a substrate and investigate the effects of electron exposure on graphene.

Fig. 2a shows an optical image of the graphene sample on hBN (sample II) which was prepared as described in the experimental section. Fig. 2b shows an AFM image of the sample, showing how the graphene was patterned. In the right hand image the area that was exposed to electrons is indicated in black. The wrinkles in the graphene are a result of the transfer process. These wrinkles do not influence results and conclusions in this paper, as can be inferred from the absence of a D peak in the Raman spectrum in Fig. 3a. The characteristic G and 2D peaks of graphene are clearly visible, with the 2D/G ratio being larger than 1. It should be noted that the increasing background in the spectrum comes about due to the underlying hBN. For comparison the Raman spectrum of a pure hBN sample is also plotted in Fig. 3a. In addition to the hBN peak at approximately 1366 cm^{-1}, the spectrum still shows the characteristic peaks of the underlying silicon at approximately 520 cm^{-1} and 970 cm^{-1}. This sample was exposed to the electron beam in the SEM in a manner identical to that detailed in the previous experiment (Fig. 2b). The dose and beam parameters were also maintained the same. The post exposure Raman spectrum (Fig. 3b) looks markedly different from that of graphene on SiO_x. It can be seen by fitting a Lorentzian function to the peak at 1366 cm^{-1} (Fig. 5b) that no D peak emerged as a consequence of electron beam induced disorder. Further, the G and 2D peaks are still intact, with the 2D/G ratio larger than 1. This suggests that electron exposure did not result in damage to graphene when hBN was used as the substrate.

In order to achieve the goal of fabricating structures on graphene using EBID, a graphene sample on hBN (sample III) was exposed to the electron beam in the presence of the organometallic precursor $MeCpPtMe_3$ (CAS number 94442-22-5) in the SEM. This sample was prepared by CVD of graphene on hBN as described in the experimental section. This sample was also wrinkled as a result of the transfer process. The chamber pressure was $1{\cdot}10^{-5}$ mbar during patterning and all other parameters used, including the dose, were the same as before. Fig. 4a shows an optical image of the graphene sample after the patterning of four structures using EBID. The deposits are known to comprise platinum grains in a carbon matrix, as a result of electron beam induced dissociation of the precursor gas used.

The post-EBID Raman spectrum of the sample (Fig. 4b) shows the characteristic G and 2D peaks, indicating that the graphene is intact. There are however some remarkable features. The 2D peak is now much lower in intensity than the G peak. It is interesting to note that such an intensity reversal has been observed after electron exposure [8] at very high electron doses (56 $\mu C/\mu m^2$).

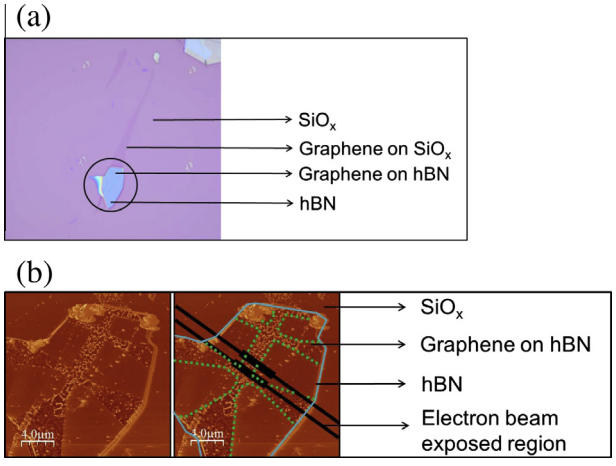

Fig. 2. (a) Optical image of the graphene sample on hBN (sample II) (b) AFM image of sample II. The black regions in the right image indicate the area that was exposed to the electron beam (dose of 20 $nC/\mu m^2$).

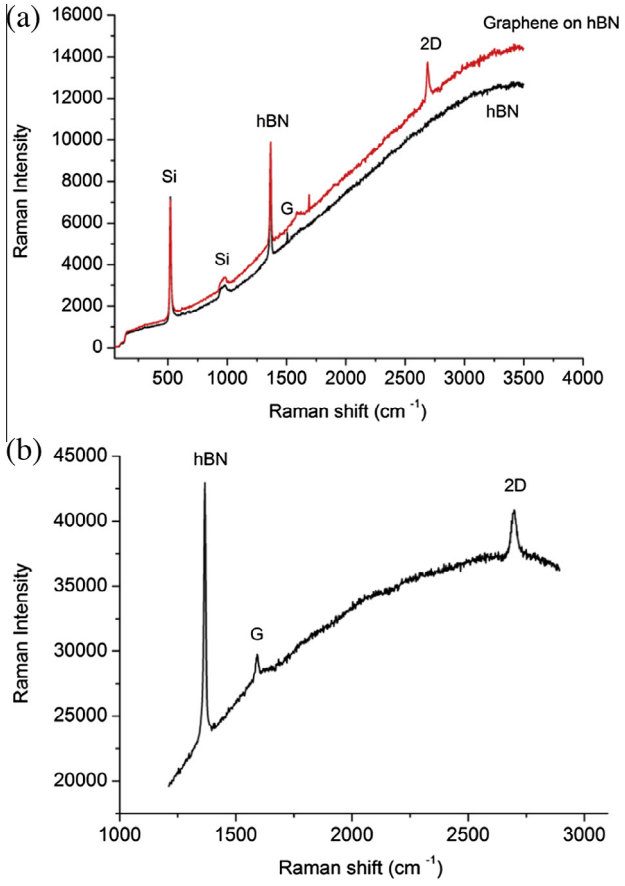

Fig. 3. (a) Raman spectrum of sample II on hBN (upper data) together with the spectrum of a pure hBN sample (lower data). The high background is due to hBN. (b) Raman spectrum of sample II after electron beam exposure.

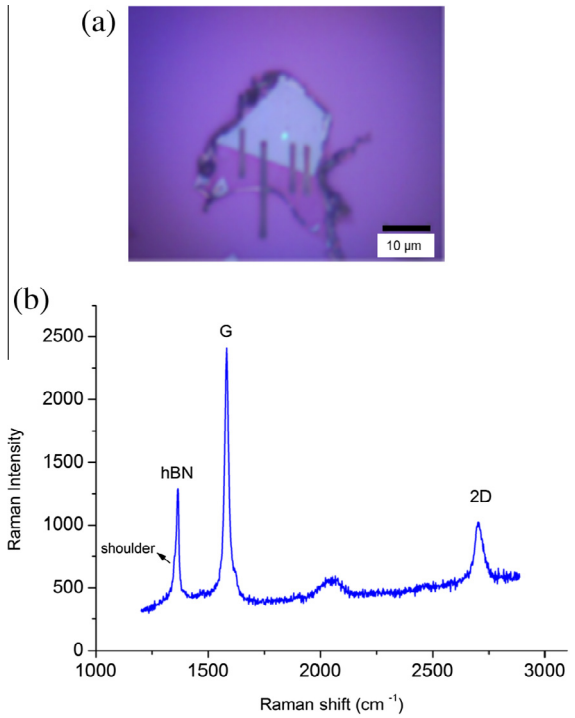

Fig. 4. (a) Optical image of graphene on hBN (sample III) after EBID patterning. The four dark lines are the EBID deposits, made up of platinum grains in a carbon matrix as a result of electron beam induced dissociation of the precursor $MeCpPtMe_3$. (b) Raman spectrum of graphene on hBN (sample III) after EBID.

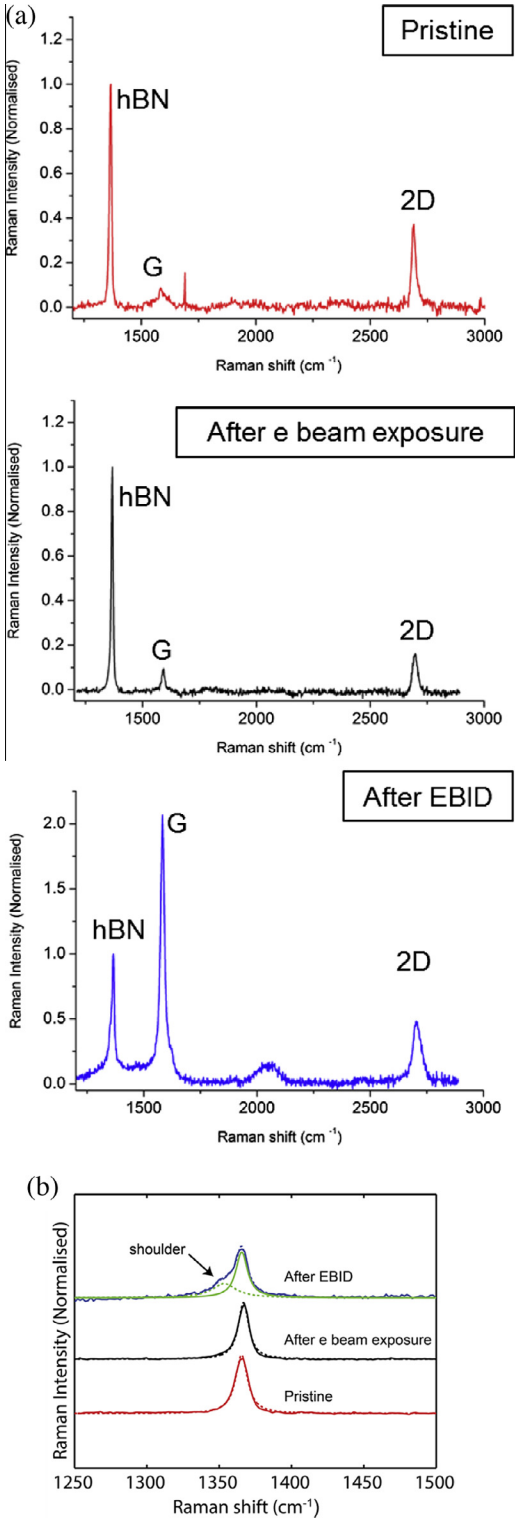

Fig. 5. (a) Raman spectrum of graphene on hBN (after background subtraction and normalizing to the hBN peak) for comparison of the pristine, post-electron exposure and post-EBID samples. Note the vertical scale difference of the lower graph compared to the upper two graphs. (b) Normalized Raman spectrum, after background subtraction, of graphene on hBN in the range 1250–1500 cm^{-1} (around the hBN peak). For clarity, the peaks are displaced in the vertical direction by an arbitrary amount. A single Lorentzian fit for the pristine sample and for the electron irradiated sample are shown (dashed lines). After EBID, the sample shows a shoulder in the hBN peak (at 1366 cm^{-1}), possibly resulting from a D peak at 1354 cm^{-1}, as revealed by the fit of two Lorentzian functions (the dashed and drawn lines shown in green online). The resultant fit (the dashed line shown in blue online) is also indicated. (For interpretation of the references to color in this figure legend, the reader is referred to the web version of this article.)

Since the dose used in our experiment was much lower, we suspect that this effect comes about not due to the electron beam exposure only (because it would have shown up in Fig. 3b), but from the introduction of the precursor gas which also contains carbon. Although the exact mechanism responsible for this is not clear, a 2D/G ratio < 1 was also observed post-EBID by Michalik et al. [9] at doses similar to that used by us.

The 2D peak appears somewhat altered after EBID. It is two times as broad and is shifted upwards by approximately 15 cm^{-1} with respect to the pristine sample (2690 cm^{-1}). There is also a peak visible around 2047 cm^{-1}, a signature of linear carbon chains [22], and a possible contribution from a broad peak extending from 1500 cm^{-1} to lower wave numbers, which is a signature of amorphous carbon [23]. Once again, this could be a result of an electron stimulated process involving the adsorbed precursor gas, such as the deposition of a thin carbon layer. In Fig. 5a we show for comparison, after background subtraction and normalizing to the hBN peak height, the Raman spectrum of the pristine sample together with the spectra of the post-electron exposure and post-EBID samples. The FWHM of the peak at 1366 cm^{-1}, attributed to hBN in the pristine sample, is approximately 7 cm^{-1} broader after EBID, with a shoulder present at the lower wave numbers. Fig. 5b shows the Raman spectrum in this range for comparison purposes, before and after exposure and after EBID, and after background subtraction and normalization to the hBN peak. Although a single Lorentzian fit to this peak still proved to be satisfactory, it was possible to carry out a fit comprising two Lorentzian functions (Fig. 5b), revealing a possible D peak at 1354 cm^{-1} in addition to the hBN peak. However, the D/G ratio in this case is 0.4, indicating a much smaller degree of damage than that induced on SiO_x (D/G = 1) due to electron exposure. Since there is no contribution from the D peak visible in the sample on hBN post electron irradiation (as can be seen from the corresponding Lorentzian fit in Fig. 5b), it is likely that this comes about due to the interaction of the electron beam with the sample in the presence of the precursor gas.

4. Conclusions

Using Raman spectroscopy, we have shown that graphene on hBN is not damaged by electron exposure at a typical EBID electron dose of 20 $nC/\mu m^2$, whereas graphene on SiO_x is. The atomic flatness of graphene on hBN as well as the absence of oxygen atoms in the substrate in this case could explain the lower degree of electron beam induced damage in graphene on hBN. Furthermore we have demonstrated that after patterning structures on graphene on hBN using EBID, the Raman spectrum of graphene still shows the characteristic features. Although changes in the peak intensities are observed and a slight degradation induced by the precursor gas might be present, the damage induced on hBN is much less than on SiO_x as can be seen by comparing the D/G ratio in the two cases. We suggest that hBN is therefore a better substrate than SiO_x for patterning graphene using an electron exposure dose in the range of 20 $nC/\mu m^2$ and even using EBID, i.e. in the presence of a precursor gas.

Acknowledgements

This work was financed in part by NanoNextNL and the authors gratefully acknowledge help from P. Kruit, V.E. Calado and R.J. Moerland.

References

[1] A.K. Geim, Science 324 (5934) (2009) 1530–1534.
[2] A.A. Balandin, Nat. Mater. 10 (2011) 569–581.
[3] D.L. Nika, A.A. Balandin, J. Phys. Condens. Matter 24 (2012) 233203.
[4] N. Silvis-Cividjian, C.W. Hagen, Adv. Imaging Electron Phys. 143 (2006) 1–235.
[5] I. Utke, P. Hoffmann, J. Melngailis, J. Vac. Sci. Technol. B 26 (2008) 1197.
[6] D. Teweldebrhan, A.A. Balandin, Appl. Phys. Lett. 94 (2009) 013101, 95 (2009) 246102.
[7] I. Childres, L.A. Jauregui, M. Foxe, J. Tian, R. Jalilian, I. Jovanovic, Y.P. Chen, Appl. Phys. Lett. 97 (2010) 173109.
[8] M. Xu, D. Fujita, N. Hanagata, Nanotechnology 21 (2010) 265705.
[9] J.M. Michalik, S. Roddaro, L. Casado, M.R. Ibarra, J.M. de Teresa, Microelectron. Eng. 88 (2001) 2063.
[10] J.D. Jones, P.A. Ecton, Y. Mo, J.M. Perez, Appl. Phys. Lett. 95 (2009) 246101.
[11] G. Liu, D. Teweldebrhan, A.A. Balandin, IEEE Trans. Nanotechnol. 10 (4) (2011) 865.
[12] A.A. Balandin, Nat. Nanotechnol. 8 (2012) 549–555.
[13] Md.Z. Hossain, Sergey Rumyantsev, Michael S. Shur, A.A. Balandin, Appl. Phys. Lett. 102 (2013) 153512.
[14] A. C. Ferrari, J. Robertson, Phys. Rev. B 61 (2000) 14095 , 64 (2001) 075414.
[15] C.O. Girit, J.C. Meyer, R. Erni, M.D. Rossell, C. Kisielowski, L. Yang, C.-H. Park, M.F. Crommie, M.L. Cohen, S.G. Louie, A. Zettl, Science 323 (2009) 1705.
[16] G.F. Schneider, V.E. Calado, H. Zandbergen, L.M.K. Vandersypen, C. Dekker, Nano Lett. 10 (2010) 1912.
[17] C.R. Dean, A.F. Young, I. Meric, C. Lee, L. Wang, S. Sorgenfrei, K. Watanabe, T. Taniguchi, P. Kim, K.L. Shepard, J. Hone, Nat. Nanotechnol. 5 (2010) 722.
[18] A.V. Baranov, A.N. Bekhterev, Y.S. Bobovich, V.I. Petrov, Opt. Spectrosc. 62 (1987) 612.
[19] C. Thomsen, S. Reich, Phys. Rev. Lett. 85 (2000) 5214.
[20] M. Yamamoto, T.L. Einstein, M.S. Fuhrer, W.G. Cullen, ACS Nano 6 (2012) 8335–8341.
[21] G. Giovannetti, P.A. Khornyakov, G. Brocks, P.J. Kelly, J. van den Brink, Phys. Rev. B 76 (2007) 073103.
[22] A.C. Ferrari, J. Robertson, Philos. Trans. R. Soc. Lond. A 362 (2004) 2477.
[23] A.C. Ferrari, Solid State Commun. 143 (2007) 47.